

LEWIS CENTER

IN-35

87908

559

NASA Contractor Report 179637

Optical Strain Measuring Techniques for High Temperature Tensile Testing

(NASA-CR-179637) OPTICAL STRAIN MEASURING
TECHNIQUES FOR HIGH TEMPERATURE TENSILE
TESTING (Cleveland State Univ.) 55 p
Avail: NTIS HC A04/MF A01 CSCL 14B

N87-26327

Unclas
G3/35 0087908

John Z. Gyekenyesi and John H. Hemann
Cleveland State University
Cleveland, Ohio

June 1987

Prepared for
Lewis Research Center
Under Grant NAG 3-749



INTRODUCTION

Ceramic composites are presently being developed for high temperature use in heat engine and space power system applications. The operating temperature range is expected to be 1090°C to 1650°C (2000°F to 3000°F). Very little material data is available at these temperatures and, therefore, it is desirable to thoroughly characterize the basic unidirectional fiber reinforced ceramic composite. This includes testing mainly for mechanical material properties at high temperatures. The proper conduct of such characterization tests requires the development of a tensile testing system in preference to flexural tests. This tensile testing system includes unique gripping, heating, and strain measuring devices which require special considerations. The system also require an optimized specimen shape.

The purpose of this paper is to review various techniques for measuring displacements or strains, preferably at elevated temperatures. Due to current equipment limitations it is assumed that the specimen is to be tested at a temperature of 1430°C (2600°F) in an oxidizing atmosphere. For the most part, previous high

temperature material characterization tests, such as flexure and tensile tests, have been performed in inert atmospheres. Due to the harsh environment in which the ceramic specimen is to be tested, many conventional strain measuring techniques can not be applied. Available methods for measuring strain or displacement include using strain gages (refs. 1 to 3), the crosshead displacement (ref. 4) of a tensile testing machine, mechanical extensometers (refs. 5 to 7), or various optical methods (ref. 8 to 77). Shown in Fig. 1 is an idealized stress-strain curve for a ceramic composite. From room temperature tensile tests of silicon carbide fiber reinforced silicon nitride (ref. 78) it has been shown that for the selected material, first matrix cracking occurs at approximately 0.1 percent strain. For the same specimen, the ultimate strength of the same material occurs at approximately 0.5 to 0.6 percent strain. The main areas of concern are the linear elastic region followed by the matrix cracking, nonlinear regime up to the ultimate strength.

Initially a brief description of the more commonly used mechanical strain measuring techniques is given. Major advantages and disadvantages with their application to high temperature tensile testing of ceramic composites are discussed. Next, a general

overview is given for various optical techniques. Advantages and disadvantages which are common to these techniques are noted.

The optical methods for measuring strain or displacement are categorized into two sections. These include real-time techniques and non-real-time, full-field techniques. Finally, an optical technique which offers optimum performance with the high temperature tensile testing of ceramic composites is recommended.

CURRENTLY USED TECHNIQUES FOR MEASURING STRAIN

Currently, many of the strain measuring methods applied to high temperature material characterization tests are mechanical. These techniques include strain gages, mechanical extensometers, and the crosshead displacement measurement method.

Strain gages are well developed, widely used, and offer low cost. In general, strain gages are simple to install and offer adequate accuracy. Unfortunately, strain gages are intolerant to elevated temperatures. At present, the highest attained working temperature is approximately 800°C (1470°F) (ref. 3). It is known that at elevated temperatures, problems with attachment of the gage to the specimen and oxidation are encountered. In addition, there are problems with the attachment of electrical leads. Thermal compensation is also difficult, resulting in subsequent lower accuracy.

Mechanical extensometers can be applied at high temperatures and they offer adequate accuracy. This technique usually requires divots or notches to be cut in the specimen surface as shown in Fig. 2. The notches or divots may cause significant stress concentrations in a specimen which can initiate first matrix cracking.

Recently, the Instron Corporation marketed an extensometer system which does not require any divots in the specimen surface. Instron's system has a light pressure applied to the extensometers to hold them against the specimen surface. Problems which may be encountered include slipping of the extensometers during a test or breaking of the quartz rods when the specimen fractures (refs. 6 to 7). The breaking of the extensometers can become quite costly with the testing of a large number of specimens. The extensometers can also act as a heat sink which would cause undesirable thermal gradients within the gage length of the specimen.

The crosshead displacement method is extremely simple and can be used with most tensile testing systems. It is also very inexpensive. The main disadvantage is that it offers very low accuracy. With the crosshead far removed from the specimen gage section it is difficult if not impossible to account for nonhomogenous strain in a specimen. It is also difficult to account for the strain in the load train. Consequently, this method is not suited for applications where high precision is required.

OPTICAL STRAIN MEASURING TECHNIQUES

Optical methods offer increased accuracy over the crosshead displacement technique and do not have the breaking problems of the mechanical extensometers. There are a number of different types of optical methods available for measuring strain or displacement. These include the laser interferometry (refs. 8 to 13), the electrooptical tracking (refs. 14 to 18), the speckle photography (refs. 19 to 22), the speckle interferometry (refs. 19,20,23 to 49), and the holography (refs. 24,40,50 to 60) methods. In addition, photoelastic coatings and conventional moire methods can be used to measure in-plane strain (ref. 23).

Difficulties can be encountered with the application of an optical strain measuring technique to high temperature tensile testing in an oxidizing atmosphere. Turbulence within the furnace causes variations in atmospheric density which cause the index of refraction of the air to change. For most of the optical methods the turbulence causes optical noise which can be partly accounted for. The furnace window can cause additional changes in diffraction which can also be compensated for. If an open window is used, then

the flow of hot gases just increases the turbulence. Therefore, one has to exercise caution so that the resulting optical noise from the increased turbulence does not interfere excessively with the desired measurements.

There are some optical strain measuring techniques which usually pose serious problems when applied to high temperature tensile testing. These include photoelastic coating methods, conventional moire techniques, and holography.

Photoelastic coating methods are simple, well developed, and offer adequate accuracy. This technique requires a coating to be placed directly on the specimen surface (ref. 23). The coating can be very difficult to maintain at high temperatures in an oxidizing atmosphere. As a result the photoelastic methods are limited to lower temperatures.

Conventional moire techniques require a grating to be placed directly on the specimen surface. As with the photoelastic methods, conventional moire techniques are simple and well developed. Also like the photoelastic methods, the conventional moire methods are limited to lower temperatures, due to difficulties in maintaining the grating. In one experiment, the moire technique has been applied at a

temperature of 750°C (1380°F) (ref. 61), but this is below the desired test temperature of ceramic composites.

Holography is a truly noncontact optical technique. It does not require any special preparation of the surface of the specimen and it is also extremely sensitive. For example, holographic interferometry using a helium-neon laser has a sensitivity of approximately 0.3 microns (12 microinches) (ref. 23). As a result, the system has to be isolated from any external vibrations making the installation or setting-up of the system quite tedious. The system also requires a laborious alignment of optics. Unfortunately, holography is best suited to measure out-of-plane displacements such as those usually encountered in vibration analysis (refs. 23 and 79). As a result, most holography applications are for flexural or transverse vibrational analysis of a specimen.

REAL TIME TECHNIQUES

In this section a description of the various techniques which give real time output is given. Due to availability of this real time output, all these methods can be used in a closed loop tensile testing system. Advantages and disadvantages with applications to the high temperature tensile testing of ceramic composites are given with each method. The general specifications such as typical gauge lengths, sensitivities, and ranges are also summarized.

It should be noted that these methods do not offer a full field view of the strains or displacements in a specimen. The output is just an average strain or displacement over the gauge length of the specimen. Most of these methods track two fiducial marks, with one at each end of the gage section.

The fiducial marks used with the majority of the real time techniques are flags which are either bonded or mechanically fastened to the specimen. Due to the harsh environment in which the specimen is to be tested, serious problems with flags may arise. For example, the adhesive used to bond the flags to the specimen may not hold causing the flags to slip or

even fall off the specimen. This would invalidate all the strain data from a test. On the other extreme, the flags may react with the specimen causing stress concentrations which can initiate matrix cracking in the immediate vicinity of the flags. For the mechanically fastened flags slipping may be a problem which would cause erratic data output. As with the bonded flags, the mechanically fastened flags can also react with the specimen causing undesirable stress concentrations.

1. LASER INTERFEROMETRIC STRAIN GAUGE

The laser interferometric strain gauge (LISG) (refs. 8 to 12), also referred to as the Sharpe method, consists of a single laser which illuminates two fiducial markings on the specimen. The markings reflect the laser light to either side of the incident beam where each reflected beam projects a set of interference fringes. The motion of the fringes is proportional to the change in the relative displacement of the markings on the specimen. Figure 3 shows a schematic of the LISG.

The change in the relative displacement between the markings is given by (ref. 8):

$$\Delta d = \frac{\lambda}{\sin \alpha} \frac{\Delta m_1 + \Delta m_2}{2} \quad (1)$$

Where: d = the relative displacement of the markings

m_1 and m_2 = the fringe orders

λ = the wavelength of the incident laser beam

α = the angle between the incident laser beam
and the reflected beams

The $(\Delta m_1 + \Delta m_{2r})/2$ term in equation (1) gives the mean value of the change in the fringe orders. This averaging accounts for the rigid body motions. The fringes can impinge on a screen and their movement measured manually with respect to a fiducial mark (ref. 10), or phototransistors or photoresistors can be used to sense the motion of the fringes. With the use of a minicomputer, the LISG has been applied to a closed loop tensile testing system (ref. 9). The actual updating of the strain output was approximately 30 times per second. This rate includes all the necessary computational times.

The markings consist of pyramidal shaped indentations produced by a Vicker's diamond micro-hardness indenter (ref. 8). These indentations can be placed directly into the specimen surface (ref. 9) or in the surface of a tab which can be adhesively bonded to the specimen (ref. 8). One of the requirements for the markings is that the surface of the indentations must be reflective.

The application of the Sharpe method to the testing of ceramic composites would require the use of the adhesively bonded tabs. Ceramics are hard and brittle making it difficult to place accurate Vicker's indentations directly in the specimen surface. Also,

recent observations have shown that the surface of some ceramics is translucent (refs. 62 and 63). As a result, the use of indentations directly in the specimen surface would not meet the requirement for a highly reflective surface. In addition to the unique problems associated with the use of ceramic specimens, the surrounding environment will be an oxidizing atmosphere (air) at 1430°C (2600°F). This would typically require the use of platinum tabs and a ceramic cement (ref. 8). Studies are presently being conducted on various ceramic adhesives to determine which can be used for the above application (ref. 8). The gage length can be varied from 100 microns (3.9 mils) (refs. 9 to 12) to about 800 microns (31 mils) (ref. 8). The gage length is relatively small. As a result, there is a high probability that first matrix cracking may occur outside of the selected gage section. This would prevent the strain gage from registering the sudden increase in strain due to matrix cracking.

Typical specifications for this method, when used in ceramic testing, are shown in Table I. Also shown in this table are the conditions under which the technique has been applied. The maximum range of 300 microns (12 mils) is actually limited by the resolution of the photodetectors. For values greater than 400

microns (16 mils) the fringes become too fine for the photodetectors to resolve (ref. 10). Out-of-plane displacements less than 25 microns (1 mil) do not cause any significant errors (ref. 10). The effect of convection currents have minimal effects due to the small gage length (ref. 11).

TABLE I: LASER INTERFEROMETRIC STRAIN GAGE (LISG)

(refs. 8 and 11)

ENVIRONMENT - AIR

MAXIMUM
TEMPERATURE - 1400°C (2550°F)

TARGET - PLATINUM TABS

GAGE LENGTH - 100 TO 800 MICRONS
(3.9 TO 31 MILS)

DISPLACEMENT
RANGE - 300 MICRONS (12 MILS)

RESOLUTION - 1 MICRON (39 MICROINCHES)

ERROR - 2 TO 3 PERCENT

2. OPTICAL STRAIN ANALYZER

The optical strain analyzer as used by Southern Research Institute consists of two telescopes mounted in a "piggy-back" arrangement (refs. 14 and 15) as shown in Fig. 4. The system is an electro-mechanical-optical design which tracks two flags on either end of the gauge length of a tensile specimen. The upper telescope tracks the upper flags carrying with it the lower telescope. The lower telescope at the same time tracks the lower flag. Elongation is measured as the displacement of the image in the lower telescope.

Each flag, as shown in Fig. 5, is a pair of targets on opposite sides of the specimen. Using a dual optical system with an average output minimizes any irregularities due to non-axial motion of the flags. High intensity lights are shined through the slots in the targets which are picked up by the telescopes. For high temperatures where the targets become self luminous, the high intensity lights are not required.

The lights passing through the targets from both sides of the specimen are formed on a rectangular aperture. The aperture contains small slits which pass the upper and lower edges of the light beams. An

optical chopper, shown in Fig. 6, breaks up the light into pulses with a fixed rate which a photodiode then converts to an alternating voltage. Commercial high fidelity audio amplifiers are used for distortion free high power amplification.

For high temperature tensile testing, this system has been applied to the testing of carbon/carbon composites in an inert atmosphere. The flags were made of carbon and were clamped onto the specimen using carbon fasteners. The design has been perfected to the level where the fracture point of the carbon specimen is not affected (ref. 15). In the case of a ceramic composite specimen in an oxidizing atmosphere, the flags would have to be redesigned. This includes selecting a material and finding a way to attach the flags to the specimen. As noted before, there is always the possibility of the material of the flags reacting with the specimen causing a stress concentration. On the other hand, it is possible for the flags to slip on the specimen making the data from the test invalid.

The optical strain analyzer allows a maximum displacement of 6.35 millimeters (250 mils) without any readjustment. It has a precision of 1.27 microns (50 microinches) (ref. 15). General specifications are summarized in Table II.

TABLE II: OPTICAL STRAIN ANALYZER

(ref. 15)

ENVIRONMENT	- INERT ATMOSPHERE
MAXIMUM TEMPERATURE	- >2000°C (3600°F)
GAGE LENGTH	- 30 MILLIMETERS (1.2 INCHES)
DISPLACEMENT RANGE	- 6.4 MILLIMETERS (0.25 INCHES)
RESOLUTION	- 1.3 MICRONS (51 MICROINCHES)
ACCURACY	- ±2.5 MICRONS (±98 MICROINCHES)

3. ELECTRO-OPTICAL STRAIN MEASURING DEVICE

The electro-optical strain measuring device which was used at Sandia Laboratories is shown in Fig. 7 (ref. 17). This system requires flags, which are shown in Fig. 8, with an adequate edge definition and contrast so that accurate tracking can be accomplished. As with many of the optical techniques mentioned in this paper, this strain measuring device was applied to the high temperature tensile testing of a specimen in an inert atmosphere (refs. 16 and 17). The maximum temperature was 2730°C (4940°F). The use of an inert atmosphere minimizes the degradation of the flags on the specimen. The flags used in these tests are ceramic cement nodules. The flags are located at each end of the gauge length. At high temperatures where the specimen and the furnace walls would be self luminous and the contrast between the flags and the specimen is minimized, a laser would be required to illuminate the flags. In reference 16, a 4 watt argon laser was utilized. It was also noted that a 2 watt laser may be adequate. A beam splitter would also be required so that each flag would be illuminated by a beam. In addition, a narrow band pass filter would be needed to allow only the light at the

frequency of the laser to pass through (ref. 16).

The optical trackers are digital-line-scan cameras which have arrays of silicon photodiodes. These are usually operated at 10 millisecond line scan times which correspond to a diode to diode sampling rate of 100 kilohertz. Working distance from specimen to camera lens is approximately 420 millimeters (16.5 inches). The camera is capable of tracking a target moving at 0.414 millimeters per second (16 mils per second). The trackers are mounted on a seismic stand for vibration isolation. Typical specifications are listed in Table III (ref. 16).

The use of an oxidizing atmosphere with the high temperature tensile testing of ceramic composites can cause problems at the attachment point of the flags. As noted before, the cement may not hold the flags in place invalidating any output from the test.

TABLE III: ELECTRO-OPTICAL STRAIN MEASURING DEVICE

(ref. 16)

ENVIRONMENT	- INERT ATMOSPHERE
MAXIMUM TEMPERATURE	- 2730°C (4950°F)
TARGET	- CERAMIC CEMENT NODULES
GAGE LENGTH	- >2.5 MILLIMETERS (98 mils)
DISPLACEMENT RANGE	- 4.24 MILLIMETERS (167 mils)
RESOLUTION	- 4 MICRONS (160 microinches)
ACCURACY	- ±4.14 MICRONS (±163 microinches)

4. SPLIT IMAGE OPTICAL EXTENSOMETER

The split image optical extensometer uses a single argon laser with a beam splitter. Two flags, one on each end of the gage length of a tensile specimen, each back lighted by a laser beam are used to project the gauge length upon a photo-multiplier tube. Figure 9 shows the arrangement of a system as used by Sandia Laboratories (ref. 18). The resultant image on the photomultiplier tube is a dark band within a light field. The edges of the dark band are due to the edges of the targets. Any changes in the specimen gage length will cause the width of the dark band to change. The photomultiplier tube detects any change in the width of the dark band and converts it to a voltage output. As with other optical systems, when a specimen becomes self luminous at high temperatures, optical filters are required which allow only the laser light to pass through. The flags require knife edges which have to be sharp and straight to provide a good image on the photo-multiplier tube.

Researchers at Sandia Laboratories applied this system to high temperature tensile testing of carbon in an inert atmosphere (helium). Figure 10 shows results

from their tests. The graphs relate the optical displacement with the target displacement. One graph is from a room temperature test and the other graph is from a high temperature test. The high temperature test was at 1200°C (2200°F). These graphs show how optical noise increases in significance with the increased temperature. This is due to turbulence within the furnace. There is also a slight change in slope between the two graphs which shows that the system should be calibrated at the temperature where it will be used.

This system requires at least a 0.5 watt laser. Table IV contains the general description and conditions under which the system was applied. Gauge lengths were varied from 10 to 100 millimeters (0.39 to 3.9 inches) (ref. 18). The accuracy was ± 2.5 microns (± 98 microinches) over a 25 millimeter (0.98 inch) gauge length (ref. 13).

The photodiode array is very sensitive to any changes in illumination. The use of a good laser eliminates any problems with illumination changes. For accurate output the centroid of the dark band must coincide with the center of the photodiode array. The centering process is accomplished with the use of stepper motors which move the photo-multiplier to the correct location. For ease of alignment it is important

to have all the optical components attached to screw driven mounts so that any required displacements or rotations can be obtained (ref. 18).

Applying the above described split image extensometer to the high temperature tensile testing of ceramics would require a new design for the flags. The flags would have to be modified such that the possibility of slipping is minimized. In addition, it is important to prevent the flags from causing significant stress concentrations within the specimen.

TABLE IV: SPLIT IMAGE OPTICAL EXTENSOMETER

(ref. 18)

ENVIRONMENT - INERT ATMOSPHERE

MAXIMUM
TEMPERATURE - 2200°C (3990°F)

TARGET - GRAPHITE CLAMPS

GAGE LENGTH - 10 TO 100 MILLIMETERS
(0.39 to 3.9 inches)

DISPLACEMENT
RANGE - 1 MILLIMETER (150 mils)

RESOLUTION - 2.5 MICRONS (98 microinches)

ACCURACY - ± 100 MICROSTRAIN
(25 MILLIMETER GAGE LENGTH)

5. ACCELERATED LASER-SPECKLE STRAIN GAUGE

The accelerated laser speckle strain gauge, unlike the other real time techniques mentioned in this paper, requires no flags on the specimen. The system detects speckle displacement caused by deformations of a laser illuminated object. Speckles are caused by the random interference of light reflected from various depths on a diffusely reflecting surface. Speckles are most obvious when the surface is illuminated by highly coherent light. The laser speckle strain gage works in real time due to a recently developed photodetector (ref. 64). Figure 11 shows a schematic of the general arrangement of the system. The photodetector, called a spatial filtering detector with electronic scanning facility, produces a voltage directly proportional to speckle displacement (ref. 64). It consists of an array of silicon photodiodes as shown in Fig. 12. The photodiodes are sensitive to specimen in-plane motion that is perpendicular to the photodiodes and to specimen out-of-plane motion. Out-of-plane motion of the specimen can be neglected as long as it is much smaller than the in-plane motion of the specimen.

The setup, as used in some experiments (refs. 64

to 66), consists of a 5 milliwatt helium-neon laser and a pair of detectors. A polarizer was also inserted to adjust the beam intensity to avoid saturating the detectors. The incident laser beam was set normal to the specimen surface with the detectors set at 45° from the incident beam as shown in Fig. 11. At present, this system has only been applied at room temperature. The output correlates well with that of a strain gauge as shown in Fig. 13.

The gauge length is equal to the laser spot diameter which is about 1 millimeter (39 mils). The photodiodes produce 2.84 millivolts per microstrain. The sensitivity can be a few thousandths of a detector period by interpolation, where the period or distance between the individual photodiodes is 320 microns (13 mils). The general specifications are noted in Table V. The response time is several tens of hertz which can be considered real time output.

One possible drawback of the system is that the sinusoidal output from the photodiode array has some probability of vanishing when the speckle pattern on the detector loses its spatial frequency component corresponding to the period of the detector. This would cause a discontinuity in the output. However, the problem can be overcome with the use of a microcomputer

to connect the areas of abrupt change (ref. 64).

Applying the laser speckle strain gauge to the high temperature tensile testing of ceramic composites in an oxidizing atmosphere can present a new set of problems. Recent observations have shown that the surface of some ceramics is translucent (refs. 62 and 63) which can cause certain problems with the tracking of the speckles. Oxidation of the specimen surface during the test would alter the specimen surface together with the speckle patterns causing decorrelation with the strain.

TABLE V: ACCELERATED LASER-SPECKLE STRAIN GAGE

(ref. 64)

ENVIRONMENT - AIR

MAXIMUM
TEMPERATURE - ROOM TEMPERATURE

TARGET - SPECIMEN SURFACE

GAGE LENGTH - 1 MILLIMETER (39 MILS)
(LASER SPOT SIZE)

STRAIN RANGE - 2000 MICROSTRAIN

SENSITIVITY - 3 MILLIVOLTS PER MICROSTRAIN

NON-REAL TIME, FULL FIELD TECHNIQUES

In this section, the various speckle methods will be described. As defined before, speckles are random points of interference of light reflected from various depths of a diffusely reflecting surface. These speckle methods offer a full field view allowing for the derivation of strains or displacements at any point on the surface of the specimen. However, these methods are not in real time. Since they require photographic processing, some form of spatial filtering and point by point analysis, the cycle time can be quite long. Consequently, these techniques can not be applied to a closed loop testing system. When applied to tensile testing, these techniques require very slow strain rates. Their possible advantages and disadvantages will be summarized below. Also, selected data such as displacement ranges and sensitivities will be given. For the high temperature tensile testing of ceramic composites, all these speckle techniques would require filters which allow only the laser light to pass. If the specimen surface changes enough due to oxidation during the test, a loss of speckle correlation can occur.

1. SPECKLE PHOTOGRAPHY

In speckle photography, a single divergent laser beam is used to illuminate a diffusely reflecting surface producing speckles. Next, a photograph is taken of the surface before and after deformation of the object by double exposure of the same film. A schematic is shown in Fig. 14(a) (ref. 19). The resulting negative, called a specklegram, is used to derive displacements at various points on the surface of the specimen.

Using the halo fringe method or Young's fringes method (ref. 67), a narrow beam of monochromatic light is passed through a point on the specklegram and an aperture as shown in Fig. 14(b). This projects a halo about the primary beam on a viewing surface which contains fringes that are perpendicular to the corresponding displacement of the point on the specimen surface. The displacement can be derived from the fringes although it can be difficult, since the quality of the fringes is rather poor near the outer edge of the halo.

Another technique for deriving displacements from the specklegram is the single beam method. The

specklegram is placed in a converging laser beam and a viewing surface is placed at the focal point as shown in Fig. 14(c). Again the result is a halo, except this time the whole specklegram is used. An aperture is placed in the viewing surface near the edge of the halo. Through this aperture a darkened view of the object can be seen. The surface of the object will contain a field of interference fringes proportional to the displacements over the whole surface of the object. These fringes represent the displacement component that is parallel to the line connecting the aperture and the focal point of the laser beam. Sensitivity can be varied by changing the distance between the focal point and the aperture.

A different approach was taken in reference 38. An opaque stop with two apertures of equal diameter is placed in front of the camera lens such that the apertures are symmetric about the lens axis. This is shown schematically in Fig. 14(d) and Fig. 15. A photograph is taken of a laser illuminated surface producing grid lines which are perpendicular to the line connecting the apertures. By double exposure, where the specimen is deformed between exposures, the two grids interfere producing moire fringes. Once the film is developed, the fringes can be viewed using white light although the quality of the fringes is quite poor. The

use of spatial filtering as shown in Fig. 14(e) can be used to improve fringe quality. These moire fringes are used to determine the relative displacements in the specimen. To derive strains, the displacements have to be differentiated.

In general, for speckle photography, as shown in Table VI, an approximate value for sensitivity is 0.36 microns (14 microinches) and a range of 36 microns (1.4 mils) (ref. 19). These values can be varied slightly by changing some of the geometric parameters but speckle photography is limited to relatively small displacements or strains. Speckle photography is not as sensitive as the holographic methods but still requires a complex setup and a laborious alignment of the optics. Tilt or rotation of a specimen has to be minimized since these conditions can cause total speckle decorrelation.

2. SPECKLE INTERFEROMETRY

One form of speckle interferometry has a specimen illuminated by two incident laser beams which are symmetric about the normal to the surface. Figure 14(f) shows a schematic of the setup. The two incident beams interfere producing a grating on the specimen surface. As with speckle photography, a photograph is taken before and after deformation of the specimen. The same film is used for each photograph; therefore the film is double exposed. The superposition of the gratings produces moire fringes. The quality of the fringes tends to be quite poor though the use of spatial filtering, shown in Fig. 14(e), improves the quality. As shown in Table VI, an approximate value for precision is 0.04 microns (1.5 microinches) and the range is approximately 6 microns (240 microinches). These values can be varied slightly by changing a few geometric parameters. Speckle interferometry has the same restrictions as speckle photography. The system requires a laborious alignment of optics. Total speckle decorrelation can occur with out-of-plane motion or tilt of the specimen. Speckle interferometry also produces poor quality fringes.

Another form of speckle interferometry is one in which the speckle pattern is sheared. In reference 35, the authors introduced a double aperture camera where a prism was placed in front of each aperture. The camera is known as a double aperture speckle shearing camera (DASSC). A schematic is shown in Fig. 16. Only a single laser beam is used to illuminate the specimen surface. The camera offers improved fringe quality, increased flexibility, and a relatively simple setup compared with other speckle methods. The DASSC does not require the vibration isolation of other speckle methods. In addition, it allows for the direct determination of strain (ref. 23). The speckle shearing method also uses double exposure of film to produce moire fringes and also requires spatial filtering. On the other hand, the use of the DASSC requires much more computing work to derive the strains from the specklegram. The range and precision of the speckle shearing technique is similar to that of speckle interferometry.

TABLE VI (ref. 19)

SPECKLE PHOTOGRAPHY

DISPLACEMENT
RANGE - 36 MICRONS (1.4 MILS)

PRECISION - 0.36 MICRONS (14 MICROINCHES)

SPECKLE INTERFEROMETRY

DISPLACEMENT
RANGE - 6 MICRONS (240 MICROINCHES)

PRECISION - 0.04 MICRONS (1.6 MICROINCHES)

CONCLUSIONS

Many of the currently available optical strain measuring techniques have been surveyed and evaluated. For the application of these techniques to the high temperature tensile testing of ceramic composites in an oxidizing atmosphere many compromises have to be made. Decisions have to be made on the primary requirements such as real time or non-real time operation, gauge length and sensitivity. For the testing of a large number of specimens, the full field techniques may become prohibitively time consuming. Also due to the harsh environment about the specimen, oxidation of the specimen surface may be enough to limit the use of the full field techniques to excessively small durations.

Due to the relatively small range of the speckle methods, speckle decorrelation may occur once matrix cracking has commenced. Many of the real time techniques will be limited by the type of flags which can be used. Since these are optical techniques, the effects of the turbulence within the furnace have to be considered.

If a quartz window is utilized, it would be another source of diffraction. On the other hand if a

quartz window is not used, the flow of hot gases can cause significant diffraction.

For the stated objective, among the methods surveyed in this paper the optical strain analyzer offers optimum performance. The system operates in real time, has a relatively large gage length, and has adequate accuracy. The system also minimizes the effects of bending.

REFERENCES

1. Brittain, J.O., Geslin, D., and Lei, J.F., "Elevated Temperature Strain Gauges," Turbine Engine Hot Section Technology 1986, NASA Conference Publication 2444.
2. Hulse, C.O., Bailey, R.S., and Grant, H.P., "Development of a High Temperature Static Strain Sensor," Turbine Engine Hot Section Technology 1986, NASA Conference Publication 2444.
3. Hobart, H.F., "The NASA Lewis Strain Gauge Laboratory - An Update," Turbine Engine Hot Section Technology 1986, NASA Conference Publication 2444.
4. Mah, T. et. al., "High Temperature Mechanical Behaviour of Fiber Reinforced Glass Ceramic Matrix Composites," Communications of the American Ceramic Society, Sep 1985.
5. Ho, E.T.C., and MacEwen, S.R., "A Facility for Precise Measurement Of Mechanical Properties At Elevated Temperatures," Journal of Metals, Feb 1983, pp.25-29.
6. Mandell, J.F., Grande, D.H., and Dannemann, K.A., "High Temperature Testing of Glass/Ceramic Matrix Composites," ASTM Symposium, "Test Methods and Design Allowables for Fibrous Composites: Second Symposium," Phoenix, Az., Nov. 3-4, 1986.
7. Mandell, J.F., Grande, D.H., and Jacobs, J., "Tensile Behaviour of Glass/Ceramic Composite Materials at Elevated Temperatures," Gas Turbine Conference and Exhibit, May 31-June 4, 1987, ASME paper no. 87GT75.
8. Jenkins, M. G., "Ceramic Crack Growth Resistance Determination Utilizing Laser Interferometry," Ph.D. Thesis, The University of Washington, 1987.
9. Martin, J.F., and Schultz B.E. "Closed-Loop Strain Controlled Testing at Elevated Temperatures With a Non-Contacting Gage," Instrumentation in the Aerospace Industry, V29, Instrument Society of America, 1983, pp. 237-240.

10. Sharpe, W.N., Jr. "Applications of the Interferometric Strain/Displacement Gage," Optical Engineering, V21, N3, May/June 1982
11. Sharpe, W.N., Jr. "In-Plane Interferometric Strain/Displacement Measurement at High Temperatures," Proceedings of the International Conference, British Society for Strain Measurement, Aug 31- Sept 4, 1981
12. Altiero, N.J., Jr., and Sharpe, W.N., Jr. "Measurement of Mixed-Mode Crack Surface Displacements and Comparison With Theory," NASA Final Report, Grant NSG-3101, Sep. 5, 1978.
13. Packman, P.F., "The Role of Interferometry in Fracture Studies," Experimental Techniques in Fracture Mechanics, 2, ed. Albert S. Kobayashi. Ames, Iowa: The Iowa State University Press.
14. Starrett, H.S., "High Temperature Tensile Testing in Air," Inter Agency Planning Group Meeting at the Institute for Defense Analysis, Alexandria, Virginia, Nov. 12, 1986.
15. Pears, C.D., et. al. "Test Methods for High Temperature Materials Characterization," Technical Report AFML-TR-79-4002
16. Marion, R.H., "A New Method of High-Temperature Strain Measurement," Experimental Mechanics, Apr 1978, pp. 134-140
17. Marion, R.H., "A Short-Time, High Temperature Mechanical Testing Facility," Journal of Testing and Evaluation, JTEVA, V6, N1, Jan 1978, pp. 3-8
18. Thompson, R.A., Jorgenson, W.E., and Callabresi, M.L., "An Optical Technique for Strain Measurement of Material Specimens at Elevated Temperatures," Sandia Laboratories Technical Publication SAND75-8261, Sep 1975.
19. Parks, V.J., "The Range of Speckle Metrology," Experimental Mechanics, June 1980, pp. 181-191.
20. Stetson, K.A., "A Review of Speckle Photography and Interferometry," Optical Engineering, V14, N5, Sep-Oct 1975, pp. 482-489.

21. Stetson, K.A., "The Vulnerability of Speckle Photography to Lens Aberrations," J. Opt. Soc. Am., V67, N11, Nov 1977, pp. 1587-1590.
22. Pollack, F.G., "Summary of Laser Speckle Photogrammetry for HOST," Turbine Engine Hot Section Technology 1986, NASA Conference Publication 2444
23. Daniel, I.M., "Optical Methods for Testing Composite Materials," In AGARD Specialist Meeting on Failure Modes of Composite Materials, 1975.
24. Funnel, W.R.J., "Image Processing Applied to the Interactive Analysis of Interferometric Fringes," Applied Optics, V20, N18, Sep 1981, pp. 3245-3250.
25. Yatagai, T. et. al., "Automatic Fringe Analysis Using Digital Image Processing Techniques," Optical Engineering, V21, N3, May/June 1982, pp. 432-435.
26. Chien, L.C. et. al., "Manual for Extending the Laser Specklegram Technique to Strain Analysis of Rotating Components," NASA Contractor Report 167932, Nov 1982.
27. Sharma, K.D., Sirohi, R.S., and Kothiyal, M.P., "Simultaneous Measurement of Slope and Curvature with a Three Aperture Speckle Shearing Interferometer," Applied Optics, V23, N10, May 1984, pp. 1542-1546.
28. Chiang, F., and Juang, R., "Laser Speckle Interferometry for Plate Bending Problems," Applied Optics, V15, N9, Sep 1976.
29. Hung, Y.Y., and Hovanesian, J.D., "Full-Field Surface-Strain and Displacement Analysis of Three-Dimensional Objects by Speckle Interferometry," Experimental Mechanics, Oct 1972, pp. 454-460.
30. Chao, Y.J., Sutton, M.A., and Taylor, C.E., "A Simple Tool for Speckle-Shearing Interferometry," Experimental Mechanics, Nov 1981, pp. 436-440.
31. Mohanty, R.K., Joenathan, C., Sirohi, R.S., "Speckle Shear Interferometry with Double Dove Prisms," Optics Communications, V47, N1, Aug 1983, pp. 27-30.
32. Chiang, F.P., "Optical Stress Analysis Using Moire

- Fringe and Laser Speckles," Optical Engineering, V18, N5, Sep/Oct 1979, pp. 448-455.
33. Spajer, M., Rastogi, P.K., and Monneret, J., "In-Plane Displacement and Strain Measurement by Speckle Interferometry and Moire Derivation," Applied Optics, V20, N19, Oct 1981, pp.3392-3402.
34. Krishna Murthy, R., Sirohi, R.S., and Kothiyal, M.P., "Speckle Shearing Interferometry: A New Method," Applied Optics, V21, N16, Aug 1982, pp.2865-2867.
35. Hung, Y.Y., Rowlands, R.E., and Daniel, I.M., "Speckle-Shearing Interferometric Technique: A Full Field Strain Gauge," Applied Optics, V14, N3, Mar 1975, pp.618-622.
36. Hung, Y.Y., Daniel, I.M., and Rowlands, R.E., "Full Field Optical Strain Measurement Having Postrecording Sensitivity and Direction Selectivity," Experimental Mechanics, Feb 1978, pp. 56-60.
37. Hung, Y.Y., and Liang, C.Y., "Image-Shearing Camera for Direct Measurement of Surface Strains," Applied Optics, V18, N7, Apr 1979, pp.1046-1051.
38. Duffy, D.E., "Moire Gauging of In-Plane Displacement Using Double Aperture Imaging," Applied Optics, V11, N8, Aug 1972, pp.1778-1781.
39. Leendertz, J.A., "Interferometric Displacement Measurement On Scattering Surfaces Utilizing Speckle Effect," Journal of Physics E: Scientific Instruments, V3, 1970, pp.214-218.
40. Brdicko, J., Olson, M.D., and Hazell, C.R., "New Aspects of Surface Displacement and Strain Analysis by Speckle Interferometry," Experimental Mechanics, May 1979.
41. Hung, Y.Y., and Grant, R.M., "Nondestructive Testing in Production Plants by Shearography," National SAMPE Symposium and Exhibition, 27th, San Diego, California, May 4-6, 1982, Society for the Advancement of Material and Process Engineering.
42. Hung, Y.Y., and Hovanesian, J.D., "Nondestructive Testing by Speckle-Shearing Interferometry."

Symposium on Nondestructive Evaluation, 12th, San Antonio, Texas, April 24-26, 1979, Southwest Research Institute.

43. Nakadate, S., and Saito, H., "Fringe Scanning Speckle-Pattern Interferometry," Applied Optics, V24, N14, Jul 1985, pp.2172-2180.
44. Nakadate, S., Yatagai, T., and Saito, H., "Computer Aided Speckle Pattern Interferometry," Applied Optics, V22, N2, Jan 1983, pp.237-243.
45. Wykes, C., Butters, J.N., and Jones, R., "Fringe Contrast in Electronic Speckle Pattern Interferometry," Applied Optics, V20, N5, Mar 1981.
46. Nakadate, S., Yatagai, T., and Saito, H., "Digital Speckle-Pattern Shearing Interferometry," Applied Optics, V19, N24, Dec 1980, pp.4241-4246.
47. Oreb, B.F., Sharon, B., and Harihan, P., "Electronic Speckle Pattern Interferometry With a Microcomputer," Applied Optics, V23, N22, Nov 1984, pp.3940-3941.
48. Nakadate, S., Yatagai, T., and Saito, H., "Electronic Speckle Pattern Interferometry Using Digital Image Processing Techniques," Applied Optics, V19, N11, June 1981, pp.1879-1883.
49. Politch, J., "Methods of Strain Measurement and Their Comparison," Optics and Lasers in Engineering, V6, 1985, pp.55-66.
50. Personal communication with Arthur Decker, Instrumentation Div., NASA Lewis Research Center, Feb. 4, 1987.
51. Doebelin, E.O. Measurement Systems: Application and Design. New York: McGraw-Hill Book Co., 1983.
52. Stetson, K.A., and Brohinsky, W.R., "Electrooptic Holography and Its Application to Hologram Interferometry," Applied Optics, V24, N21, Nov 1985.
53. Nelson, D.V., and McCrickerd, J.T., "Residual-Stress Determination Through the Use of Holographic Interferometry and Blind-Hole Drilling," Experimental Mechanics, Dec 1986, pp. 371-378.

54. Gilbert, J.A., "Differentiation of Holographic-Moire Patterns," Experimental Mechanics, Nov 1978, pp. 436-440.
55. Decker, A.J., "Beam-Modulation Methods in Quantitative and Flow-Visualization Holographic Interferometry," NASA Technical Memorandum 87306.
56. Katzir, Y., and Glaser, I., "Separation of In-Plane and Out-of-Plane Motions in Holographic Interferometry," Applied Optics, V21, N4, Feb 1982, pp. 678-683.
57. Nakadate, S. et. al., "Hybrid Holographic Interferometers for Measuring Three-Dimensional Deformations," Optical Engineering, V20, N2, Mar/Apr 1981, pp. 246-252.
58. Wallach, J., Holeman, J.M., and Passanti F.A., "Holographic Strain Measurement on a Tensile Specimen," Proceedings of the Symposium, Los Angeles, California, Feb. 16-17, 1972. Society of Photo-optical Instrumentation Engineers.
59. Balas, J., Sladek, J., and Drzik, M., "Stress Analysis by Combination of Holographic Interferometry and Boundary-Integral Method," Experimental Mechanics, Jun 1983, pp. 196-202.
60. Decker, A.J., "Advanced Optical Measuring Systems for Measuring the Properties of Fluids and Structures," NASA Technical Memorandum 88829.
61. Cloud, G., Radke, R., and Peiffer, J., "Moire Grating for High Temperatures and Long Times," Experimental Mechanics, Oct 1979.
62. Personal communication with John Barranger, Instrumentation Div., NASA Lewis Research Center Dec. 1, 1986.
63. Personal communication with John Barranger, Instrumentation Div., NASA Lewis Research Center Jan. 28, 1987.
64. Yamaguchi, I., and Furukawa, T., "Accelerated Laser Speckle Strain Gauge," SPEI Vol. 556 International Conference on Speckle, 1985.

65. Yamaguchi, I., "A Laser-Speckle Strain Gauge," J. Phys. E: Sci. Instrum., Vol. 14, 1981.
66. Yamaguchi, I., "Simplified Laser-Speckle Strain Gauge," Optical Engineering, Vol. 21 No. 3, May/June 1982.
67. Parks, V.J., "A Simplified Description of Speckle Fringe Formation," In Joint Conference on Experimental Mechanics Oahu and Maui, Hi, May 23-28, 1982
68. Hercher, M., Wyntjes, G., and DeWeerd, H., "Non-Contact Laser Extensometer," International Society for Optical Engineering, Los Angeles, California, Jan. 11-16, 1987.
69. Ranson, W.F., and Sutter, J.L., "Surface Displacement Measurements Utilizing Digital Image Techniques," Submitted to NASA, Lewis Research Center through University of South Carolina, Sept. 1981.
70. Butters, J.N., "Speckle Interferometry," Optical Transducers and Techniques in Engineering Measurement. London, Applied Science Publishers, 1983, pp. 205-238.
71. Hung, Y.Y., "Displacement and Strain Measurement," Speckle Metrology, ed. Robert K. Erf. New York: Academic Press, 1978.
72. Weissmann, G.F., Carter, H.L., Jr., and Hart, R.R., "Optical Displacement Measuring Device," International Instrumentation Symposium, 25th, Anaheim, California, May 7-10, 1979, Instrument Society of America.
73. Mecholsky, J.J., "Evaluation of Mechanical Property Testing Methods for Ceramic Matrix Composites," Ceramic Bulletin, V65, N2, 1986, pp.315-322.
74. Larsen, D.C., et. al., "Test Methodology for Ceramic Fiber Composites: Results for SiC/LAS, SiC/SiC, and C/SiC Composites," In NASA, Langley Research Center Metal Matrix, Carbon, and Ceramic Matrix Composites 1985.

75. Akhavan Leilabady, P., Jones, J.D.C., and Jackson, D.A., "Monomode Fiber-Optic Strain Gauge With Simultaneous Phase and Polarization State Detection," Optics Letters, V10, N11, Nov 1985.
76. Davies, C.K.L., and Sinha Ray, S.K., "A Simple Apparatus for Carrying Out Tensile Creep Tests On Brittle Materials Up To Temperatures of 1750°C," Journal of Physics E: Scientific Instruments, V4, 1971.
77. Sevenhuijsen, P.J., "Structural Deformation: A Comprehensive Survey Of Modern Measurement Methods," National Aerospace Lab., Amsterdam (Netherlands), HC A06/MF A01, 1982.
78. Bhatt, Ramakrishna T., "Mechanical Properties of SiC Fiber-Reinforced Reaction-Bonded Si₃N₄ Composites," NASA Technical Memorandum 87085.
79. Whitney, J.M., Daniel, I.M., and Pipes, R.B. Experimental Mechanics of Fiber Reinforced Composite Materials. Brookfield Center, Conn.: The Society for Experimental Stress Analysis, 1982.

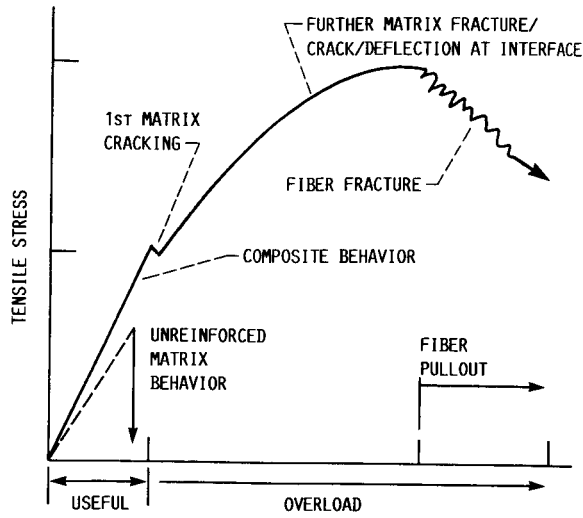


FIGURE 1. - IDEALIZED STRESS-STRAIN BEHAVIOR OF CERAMIC FIBER COMPOSITES. (REF. 74.).

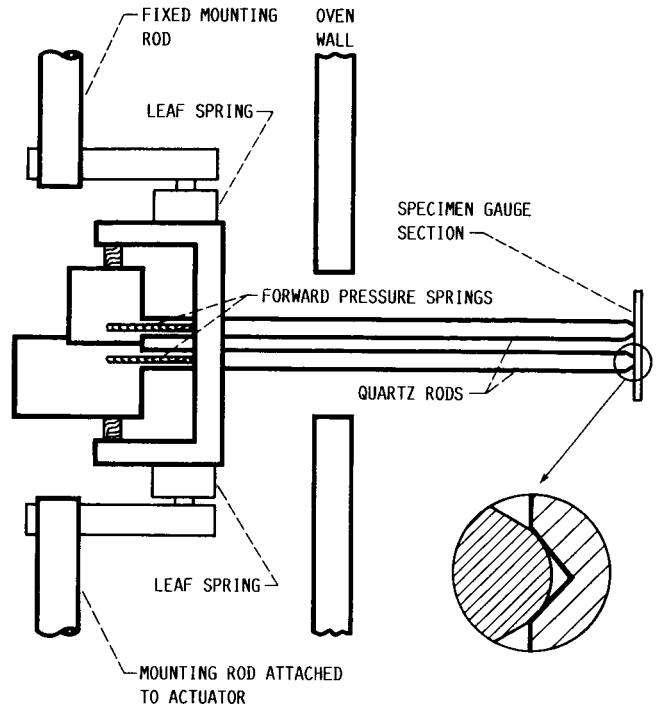
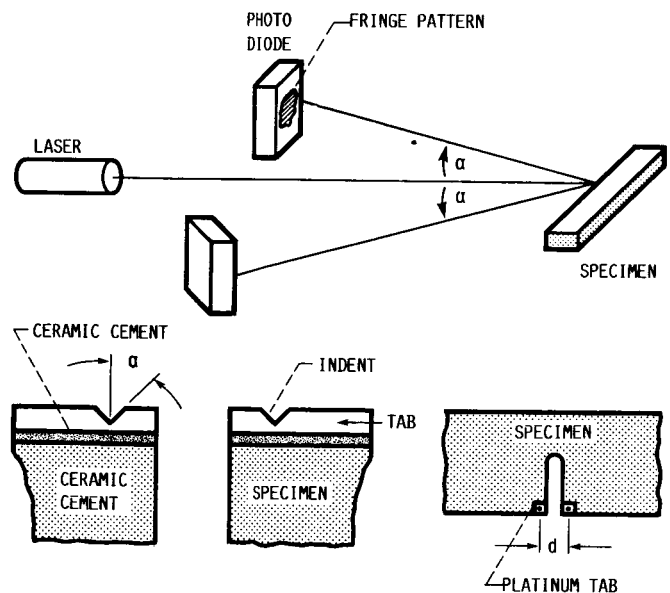


FIGURE 2. - SCHEMATIC OF LONGITUDINAL EXTENSOMETER AND DETAIL OF ROD TIP AT SPECIMEN SURFACE DIVOT. (REF. 6.).



$$\Delta d = \frac{M_1 + M_2}{2} \frac{\lambda}{\sin \alpha}$$

FIGURE 3. - SCHEMATICS OF LASER INTERFEROMETRIC STRAIN GAUGE. (REF. 8.).

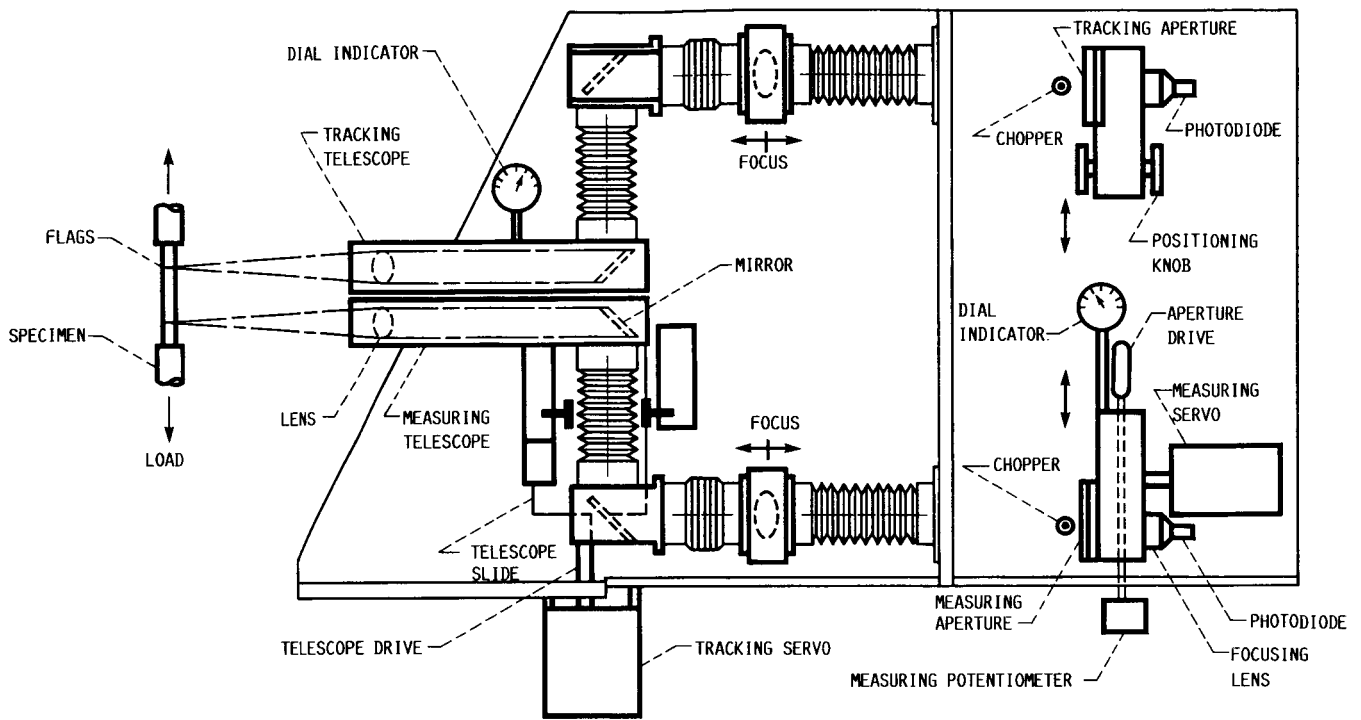


FIGURE 4. - OPTICAL STRAIN ANALYZER. (REF. 14.).

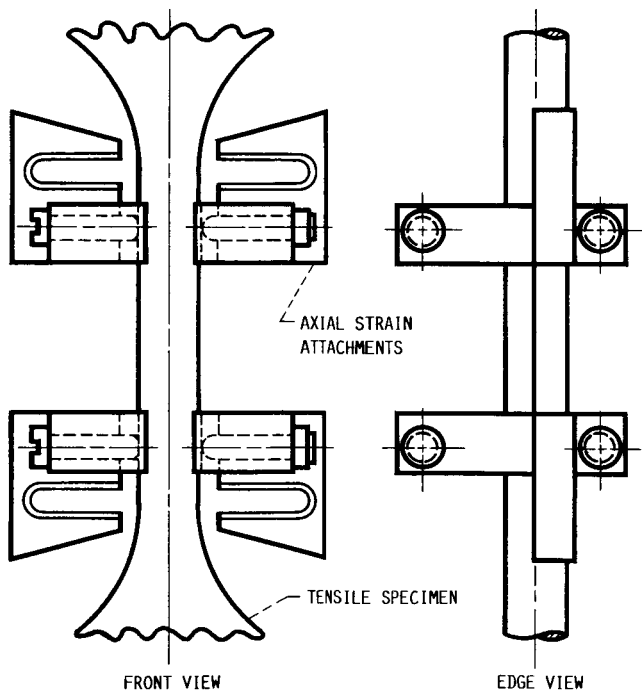


FIGURE 5. - STRAIN TARGET ATTACHMENT ON TENSILE SPECIMEN. (REF. 14.)

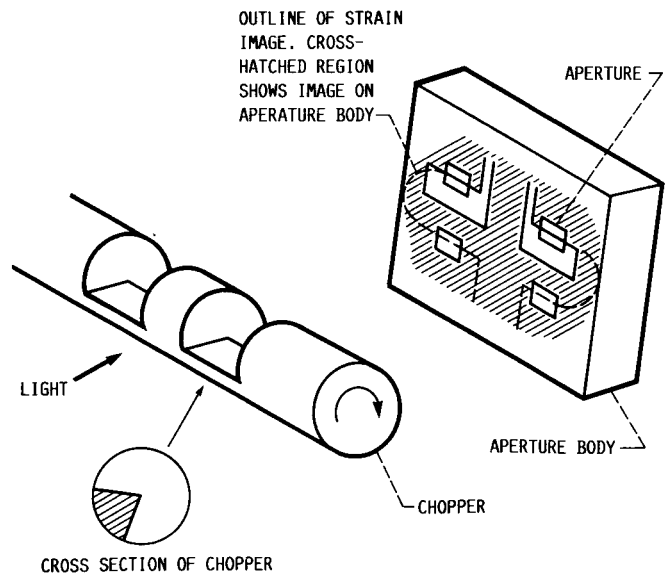


FIGURE 6. - SCHEMATIC SHOWING THE RELATIONSHIP OF THE CHOPPER TO APERTURES. (REF. 14.).

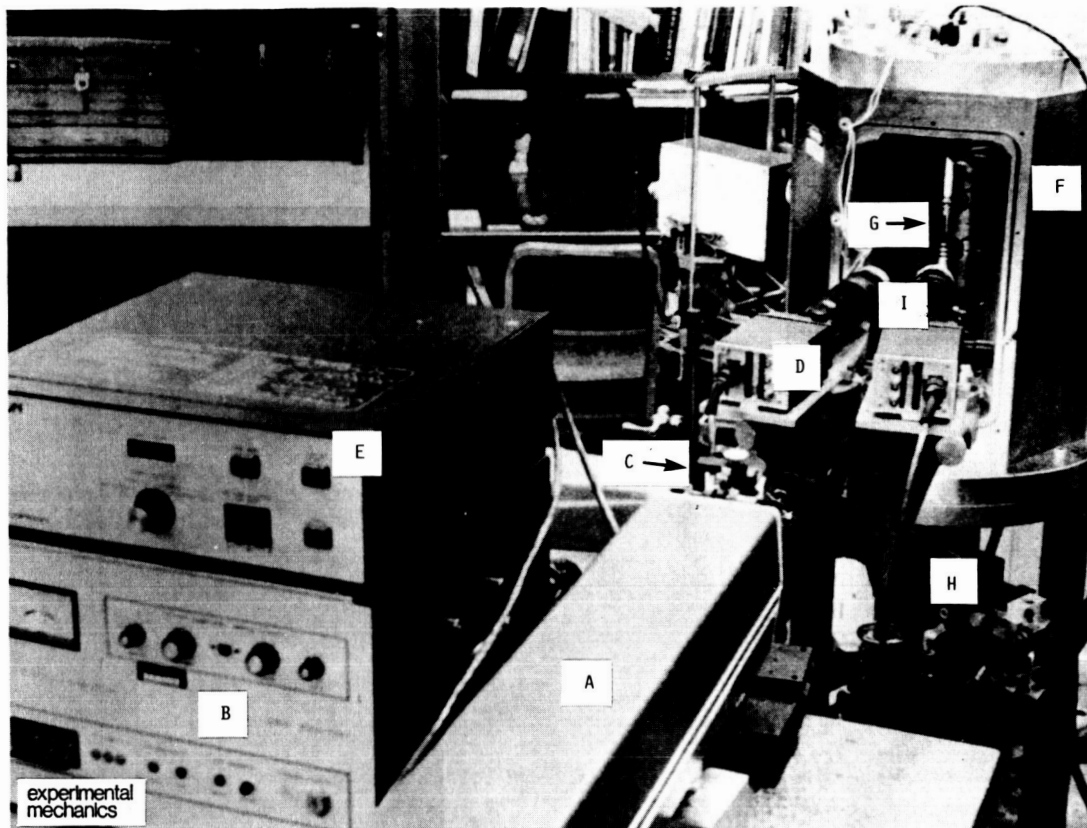


FIGURE 7. - EXPERIMENTAL SETUP: (A) LASER; (B) LASER POWER SUPPLY; (C) OPTICS FOR DIVIDING, SHAPING, AND DIRECTING LASER BEAM; (D) DIGITAL LINE SCAN TRACKER WITH LENS AND INTERFERENCE FILTER MOUNTED ON FRONT; (E) TRACKER CONTROLLER; (F) TEST CHAMBER WITH WINDOW REMOVED; (G) TEST SPECIMEN; (H) LOADING RAM; AND (I) INFRARED PYROMETER. (REF. 16.).

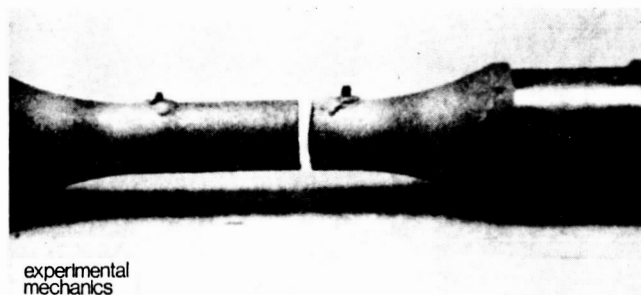


FIGURE 8. - FRACTURED ATJ(S) GRAPHITE TEST SPECIMEN SHOWING THE STRAIN-MEASUREMENT NODULES. (THE GAUGE DIAMETER IS 6.35 MM) (REF. 16.).

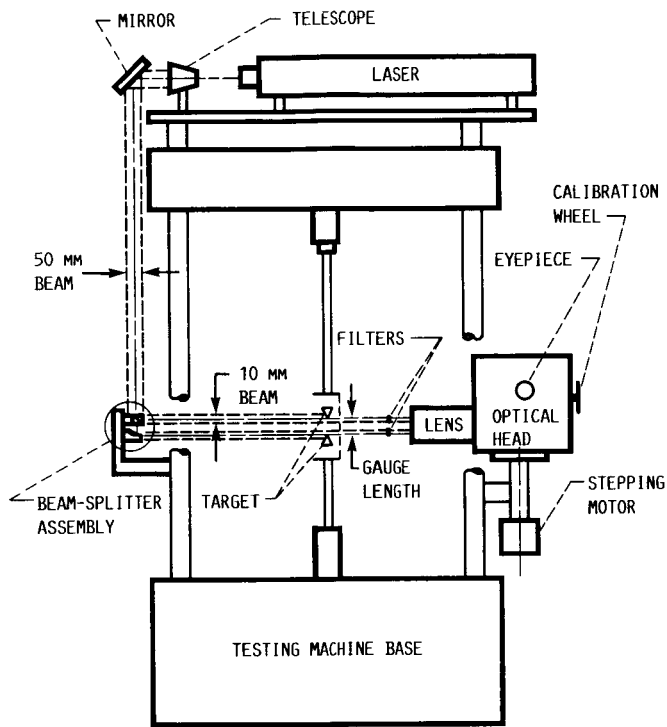


FIGURE 9. - ARRANGEMENT OF OPTICAL SYSTEM. (REF. 18.).

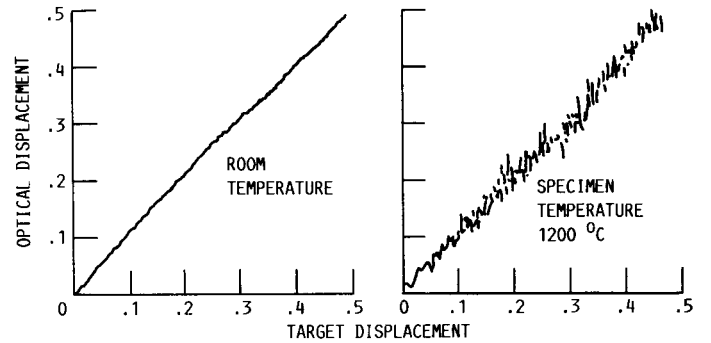


FIGURE 10. - EXPERIMENTAL RESULTS. (REF. 18.).

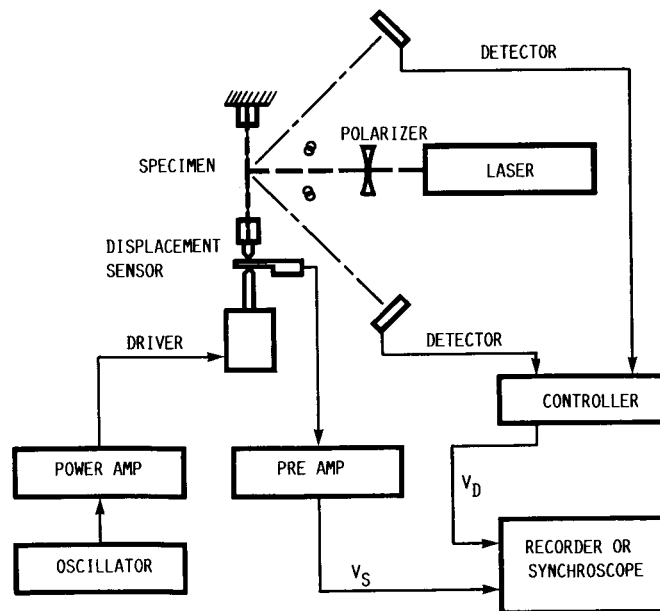


FIGURE 11. - FUNDAMENTAL ARRANGEMENT FOR MEASURING TENSILE STRAIN USING LASER SPECKLE STRAIN GAUGE. (REF. 64.).

ORIGINAL PAGE IS
OF POOR QUALITY.

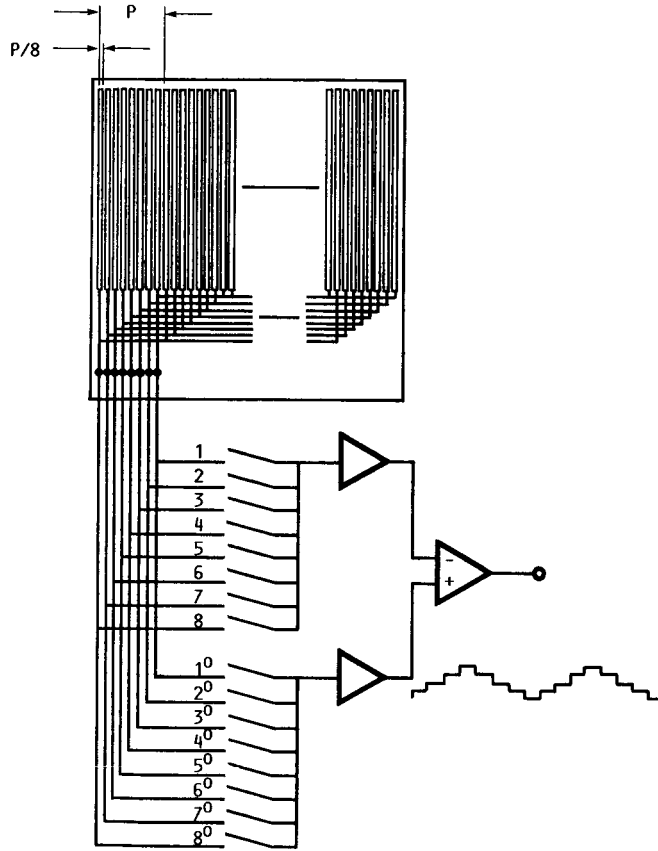


FIGURE 12. - GEOMETRY OF PHOTODIODE ARRAY AND ELECTRONIC INTERCONNECTIONS. (REF. 64.).

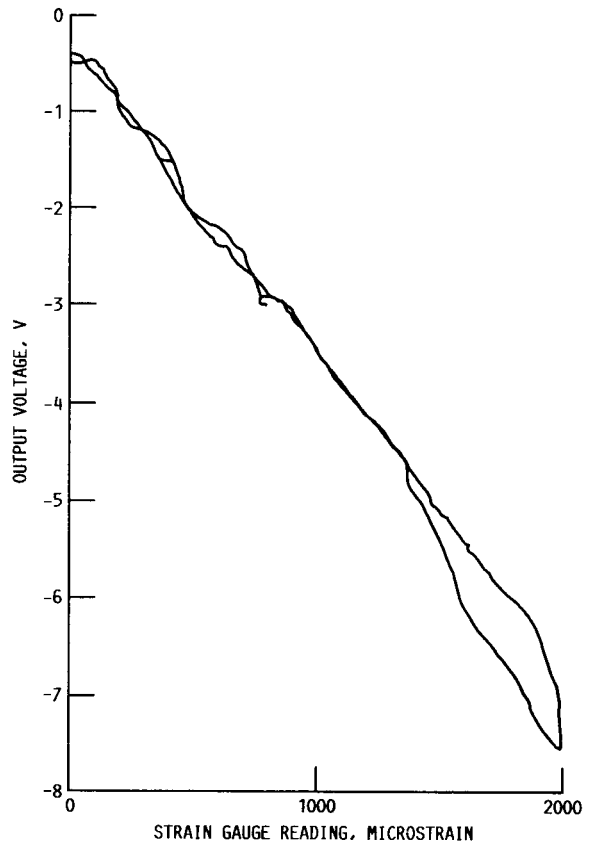


FIGURE 13. - DIFFERENTIAL VOLTAGE VERSUS OUTPUT OF A RESISTANCE STRAIN GAUGE. (REF. 64.).

$$\delta = \lambda \frac{n}{2 \sin \theta}$$

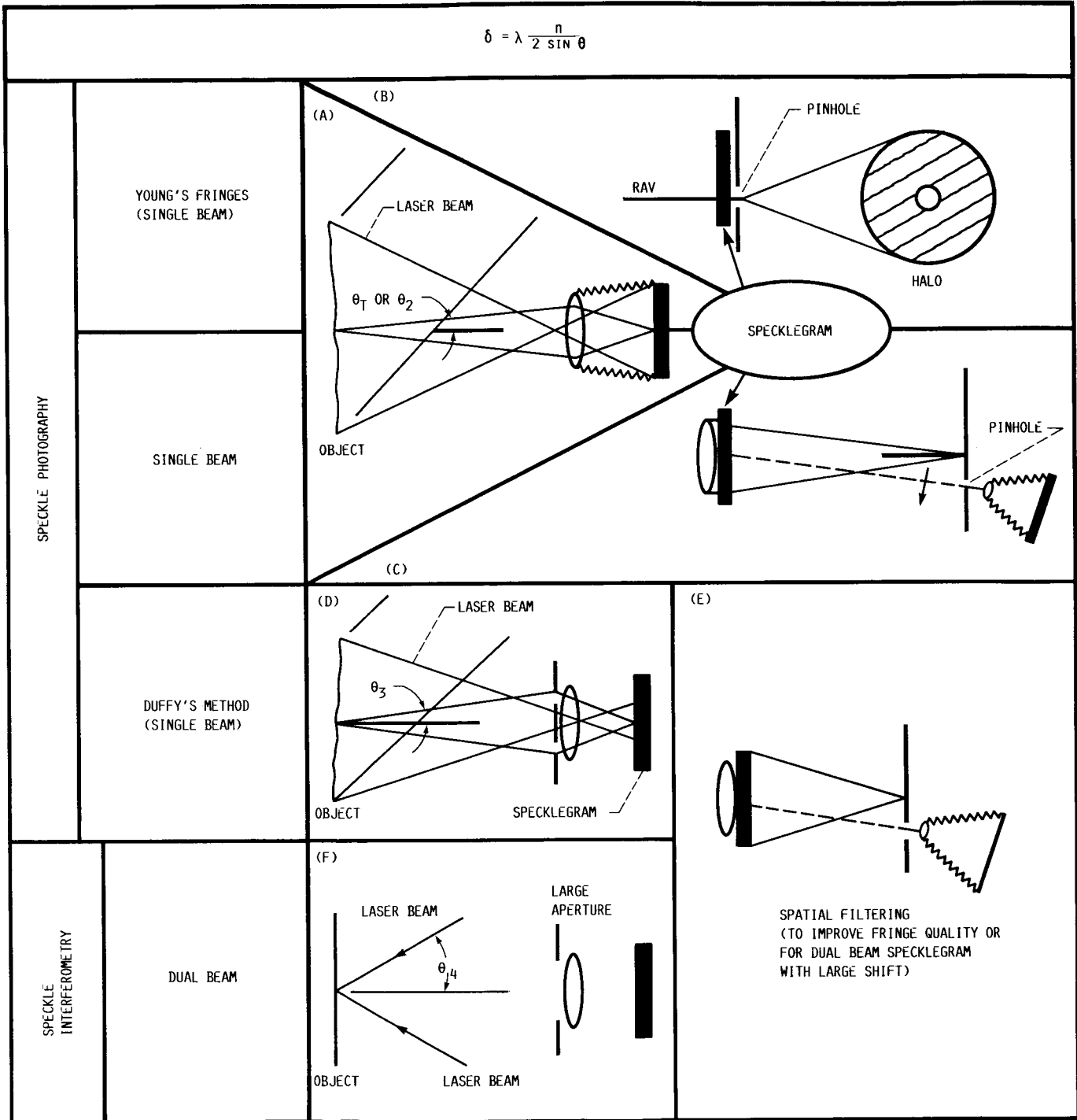


FIGURE 14. - FOUR METHODS TO PRODUCE AND ANALYZE IN-PLANE DISPLACEMENT FRINGES. (REF. 19.).

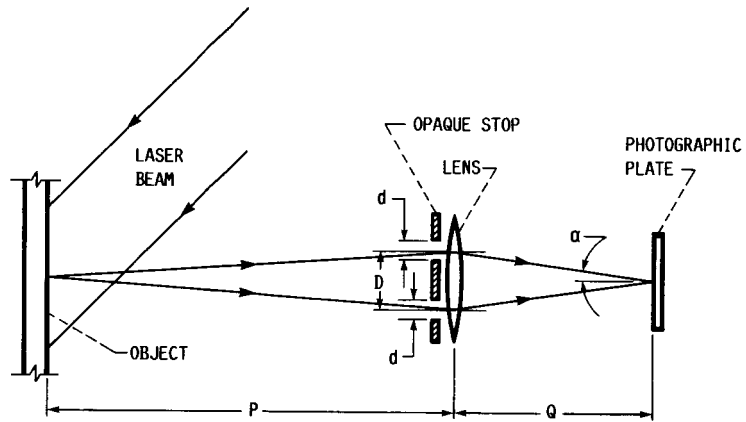


FIGURE 15. - SCHEMATIC OF DOUBLE APERTURE CAMERA.

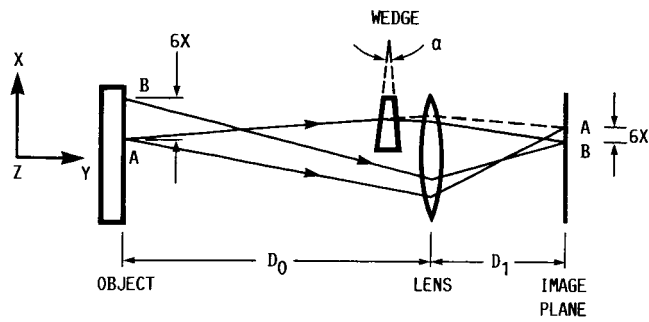


FIGURE 16. - IMAGING DETAIL OF THE IMAGE SHEARING CAMERA. (REF. 37.).



National Aeronautics and
Space Administration

Report Documentation Page

1. Report No. NASA CR-179637		2. Government Accession No.		3. Recipient's Catalog No.	
4. Title and Subtitle Optical Strain Measuring Techniques for High Temperature Tensile Testing				5. Report Date June 1987	
				6. Performing Organization Code	
7. Author(s) John Z. Gyekenyesi and John H. Hemann				8. Performing Organization Report No. None	
				10. Work Unit No. 506-43-11	
9. Performing Organization Name and Address Cleveland State University Department of Civil Engineering Cleveland, Ohio 44115				11. Contract or Grant No. NAG 3-749	
				13. Type of Report and Period Covered Contractor Report Final	
12. Sponsoring Agency Name and Address National Aeronautics and Space Administration Lewis Research Center Cleveland, Ohio 44135				14. Sponsoring Agency Code	
15. Supplementary Notes Project Manager, Frances I. Hurwitz, Materials Division, NASA Lewis Research Center.					
16. Abstract A number of optical techniques used for the analysis of in-plane displacements or strains are reviewed. The application would be for the high temperature, approximately 1430 °C (2600 °F), tensile testing of ceramic composites in an oxidizing atmosphere. General descriptions of the various techniques and specifics such as gauge lengths and sensitivities are noted. Also, possible problems with the use of each method in the given application are discussed.					
17. Key Words (Suggested by Author(s)) High temperature testing; Optical strain gage; Tensile testing; Ceramic matrix composites			18. Distribution Statement Unclassified - unlimited STAR Category 35		
19. Security Classif. (of this report) Unclassified		20. Security Classif. (of this page) Unclassified		21. No of pages 54	22. Price* A04